PHYSICAL REVIEW B

CONDENSED MATTER

THIRD SERIES, VOLUME 43, NUMBER 18 15 JUNE 1991-II

Reconstruction of the (100) surfaces of Au and Ag

Noboru Takeuchi, C. T. Chan, and K. M. Ho

Ames Laboratory and Department of Physics, Iowa State University, Ames, Iowa 50011

(Received 14 February 1991)

Using first-principles total-energy calculations, together with simulations performed with a Frenkel-Kontorowa model, we show that it is energetically favorable for the top layer of the (100) surface of Au to transform from the ideal square lattice of the (100) surface of a fcc metal to a slightly distorted and contracted hexagonal-close-packed arrangement. The ground-state configuration from our simulation agrees well with experimental observations. The reconstruction is shown to be unfavorable in Ag, which is isoelectronic to Au. The difference in behavior is because the two-dimensional Au layer gains much more energy upon contraction than its Ag counterpart.

I. INTRODUCTION

The structure of gold surfaces has been studied extensively using different experimental techniques.[1-13] It has been known for many years that the low-index surfaces of gold reconstruct. In particular, the Au(100) surface exhibits a complex reconstruction pattern. The ideal unreconstructed (100) surface of Au should be a square lattice, but experiments indicate that the ground state of this surface corresponds to a contracted hexagonal-close-packed overlayer on top of a square substrate. Early low-energy electron-diffraction (LEED)[1] and He-scattering[2] measurements of this surface indicated a (1×5) reconstruction. Later LEED measurements resolved the splitting in the LEED spots, suggesting a (20×5) rather than a (1×5) superstructure.[3] Other LEED[4] studies suggested a larger $c(26\times68)$ unit cell. Bining, Rohrer, Gerber, and Stoll,[5] using scanning tunneling microscopy, proposed a

$$\begin{bmatrix} X & 0 \\ Z & Y \end{bmatrix}$$

unit cell, where $X=24\pm3$, $Y=48$ or 43, depending on temperature, and $-5\leq Z\leq 0$, implying an additional rotation of the overlayer over the substrate. A recent study of the temperature dependence of the Au(100) surface structure[13] found a distorted hexagonal structure for 970 K $< T <$ 1170 K and a rotated distorted hexagonal structure for 300 K $< T <$ 970 K. This perplexing surface layer transformation is not restricted to Au, the (100) surfaces of other 5*d* fcc metals show similar reconstructions: Ir(100) exhibits a (1×5) pattern,[3] and Pt(100) shows a series of closely related patterns with quasihexagonal unit cells, two of them have (5×1) and (5×20) structures.[4] On the other hand, the isoelectronic 4*d* fcc metals Rh, Pd, and Ag do not show any reconstruction on their (100) surfaces.

On the theoretical side, the Au surface reconstruction has been studied successfully by Ercolessi, Parinello, and Tossatti using a "glue model,"[14] and by Dodson using the embedded atom method.[15] These are simulations with the Au-Au interactions represented by empirical classical potentials. In this paper, we will present theoretical results from a different point of view. We put more emphasis on understanding the driving force of the phenomena, and in particular, why the reconstruction occurs in 5*d* fcc metals but not in the 4*d* metals, using Au and Ag as prototypes. To this end, we pursue the problem using first-principles total-energy techniques as much as possible. The first-principles calculations give us insight at a microscopic level, and at the same time provide us with sufficient information that allows us to extrapolate our results to the more complex phenomena using simple models. A short version of this paper has been published previously.[16]

This class of surface reconstruction, which involves the transformation of the top layer to a different symmetry, cannot be studied by *ab initio* calculations alone. The top layer is in principle incommensurate with the underlying layers. Mapping the problem into a commensurate surface cell results in a huge unit cell, much larger than what we can handle with computers currently available. Even if we can handle tens of thousands of atoms in first-principles calculations and hence treat the problem in a brute-force manner, we will probably be overwhelmed by excessive numerical information and may not be able to identify the key driving force behind the transformation. It is thus a necessity to combine *ab initio* calculations with modeling techniques in order to give a comprehen-

sive description of the phenomena.

For the observed transformation to occur, the top layer must transform to a hexagonal structure and the energy gained in the process has to be larger than the energy loss caused by the loss of registry (sometimes called the "mismatch" energy) with the underlying layers. So in the first step, we study carefully the energetics of a monolayer for both Au and Ag. We will show that for both a monolayer in isolation and a monolayer on top of a jellium slab, the ground state is a contracted hexagonal-close-packed structure for both Au and Ag; however, the gain in energy upon contraction is substantially bigger for the Au monolayer. The mismatch energy can be estimated by computing the energy of the system as the top-layer atoms are displaced (in the absence of contraction) laterally to various different surface sites. The results from the first-principles calculations are used as input data into a two-dimensional Frenkel-Kontorowa-like model to search for the ground state of the system. We will show that it is energetically favorable for the (100) surface of Au, but not for Ag, to reconstruct.

The rest of the paper is organized as follows: The first-principles calculation procedures are described in Sec. II; the energetics of Ag and Au monolayers in isolation and on top of jellium slabs are presented in Secs. III and IV, respectively. In Sec. V we present first-principles results of the top layer occupying different positions with respect to the substrate. The mapping of our first-principles results onto a two-dimensional Frenkel-Kontorowa (FK) model and the simulation using the FK model is described in Sec. VI. Finally, Sec. VII is a summary of the paper.

II. FIRST-PRINCIPLES CALCULATIONS

We used in our calculations nonlocal ionic pseudopotentials generated using the norm-conserving scheme of Hamman, Schluter, and Chiang.[17] The total energies are calculated within the local density functional formalism[18] with the Hedin-Lundqvist form[19] of the local exchange-correlation energy. The wave functions are expanded by means of an efficient "mixed-basis" set[20] consisting of plane waves with kinetic energy $(\mathbf{k}+\mathbf{G})^2$ up to 12 Ry plus a set of localized Bloch functions centered at the atomic sites to describe the d orbitals. For Au, we use a Gaussian to describe the radial part of the localized orbitals, and for Ag, due to the fact that the $4d$ states are more tightly bound than the Au $5d$ states, a numerical function is used for the radial part of the local orbitals. Numerical functions are more flexible and hence can better represent the local orbitals. The number of plane waves needed for convergence is then reduced, leading to smaller Hamiltonian matrices and hence less computation time. The shape of the local orbitals are determined variationally and details can be found in a previous publication.[21] The charge density for Au is expanded with approximately 2300 plane waves corresponding to a cutoff energy of approximately 110 Ry. For the case of Ag, we use approximately 8000 plane waves for the charge-density expansion corresponding to a cuttoff energy of 256 Ry. For most of the calculations 15 $\mathbf{k}$ points are used in the irreducible wedge of the surface Brillouin zone (SBZ), and some results are checked with larger $\mathbf{k}$-point sets. This method has been used in previous investigations of the structural properties of bulk Au and Ag (Ref. 21) and the reconstruction of the (110) (Ref. 22) and (111) (Ref. 23) surfaces with excellent results.

III. Ag AND Au MONOLAYER

On the reconstructed Au(100) surface the topmost (100) layer contracts and transforms to a hexagonal-close-packed arrangement, while deeper (100) layers remain in the bulk structure. Experiments studying the growth of a thin film of Pt on a Pd(100) substrate have shown that the addition of a single monolayer of Pt is sufficient to produce a (5×1) reconstruction pattern.[24] Also the contractions of all the (100) surfaces of the $5d$ fcc metals develop from an in-registry structure into a compressed structure. All these results suggest that the atomic interactions in the top surface layer play the dominant role in this class of reconstruction. Thus, it is reasonable to study, as the first step, the behavior of a single (100) layer by itself.

The total energy of the two-dimensional monolayer is calculated with the "supercell" technique,[25] which regains periodicity in the direction perpendicular to the surface of the monolayer by repeating the monolayers in the (100) directions, with the layers separated by a distance large enough that the influence of their mutual interaction is small for the quantities in which we are interested. Here we are interested in the relative energy of the monolayer as a function of the density and symmetry of layer. We found that a separation of 15.5 a.u. between two consecutive monolayers is large enough for our purpose. We have repeated the calculation with a smaller separation of 10.9 a.u., and results are almost identical. In our studies of Au and Ag monolayers, total energies are calculated for both square and hexagonal structures, and for each structure we varied the lattice area per atom. The results are fitted to a "universal binding curve,"[26] which have the form

$$E(a)=\Delta E\,\xi(\alpha)\ , \tag{1}$$

with $\alpha=(a-a_m)/l$, $\xi(\alpha)=(1+\alpha)\exp(-\alpha)$, where ΔE, a_m, and l are scaling parameters. The value of ΔE is the cohesive energy per surface atom (the energy with respect to the free atom),[21] the quantity α is a scaled length, a_m is the equilibrium lattice constant, and l is a scaling length related to the curvature of the total-energy curve at the equilibrium point. In Figs. 1(a) and 1(b), we plot the energy change for the Au and Ag monolayers (for both square and hexagonal symmetry) as a function of the percentage reduction of surface area per atom. The "zeros" in the contraction correspond to the area per unit atom on an ideal (100) surface, and the energy gain is with respect to the energy of the square monolayer at that area. The calculations were done with 15 $\mathbf{k}$ points in the irreducible SBZ. We check the $\mathbf{k}$-point convergence by repeating the calculation with 36 $\mathbf{k}$ points in the SBZ, and results are compared in Fig. 2 for the case of a hexagonal-Au monolayer. The nearly identical results in-

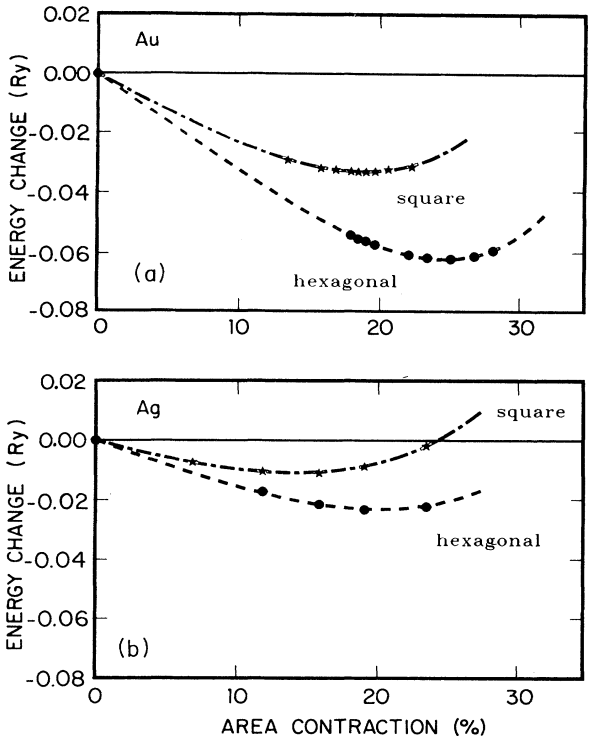

FIG. 1. Energy change per atom for square and hexagonal monolayers as a function of the percentage contraction of surface area per atom for (a) Au and (b) Ag. Zero corresponds to the area occupied per surface atom on the ideal (100) surface.

dicate good k-point convergence. We observe from Fig. 1 that for both Au and Ag monolayers, the hexagonal structure gives the lowest energy, and the minimum of the energy occurs at a surface density higher than that on an ideal (100) surface of the fcc structure. It is interesting to note that at the ground state, atoms in the monolayer are closer together than the atoms on a (111) face (the most compact surface of a fcc structure). The area per atom on the (111) planes is 13.4% smaller than that of the (100) planes. This calculation shows that there is indeed a strong inclination for the top layer itself to transform to the close-packed configuration observed in experiments. This is true for both Au and Ag, but is clear from Fig. 1 that Au contracts more and gains much more energy in the process. The area of contraction for Au is approximately 25%, larger than the 20% in the ground state of Ag. Ag gains about 23 mRy per atom in contracting and transforming, while Au gains more than 60 mRy per atom, or about 2.5 times more energy than Ag.

It is important to know the reason why the Au layer gains more energy than Ag in the transformation process. Since the d shells in the noble metals are nominally filled, the importance of the d electrons has not been taken seriously in the reconstruction of the Au(100) surface.[27] We found that the d electrons actually play a crucial role in determining the energetics of the problem, in particular, the difference between Au and Ag. The 5d electrons in Au have wave functions more extended than the 4d electrons in Ag, and the d bands in Au are closer to the Fermi level. The d electrons in Au thus contribute to the bonding and cohesion much more than Ag through hybridization with the s band. The stronger bonding from the 5d electrons manifests itself in the bulk properties: 5d fcc metals have larger cohesive energies and stiffer bulk moduli than the corresponding 4d metals. Stronger bonding is also responsible for the fact that the 5d metals have almost the same equilibrium volume as their respective 4d counterparts, even though they have bigger cores. Ho and Bohnen[22] showed that increasing the d part of the Au pseudopotential by 5%, thereby making the d states more tightly bound and less reactive, the cohesive energy and the bulk modulus of Au became much closer to those of Ag. We repeat the hexagonal-monolayer calculation using this modified Au pseudopotential, and results are shown in Fig. 3. We can see that once the d states in Au are drawn artificially closer to the nucleus by making the d part of the pseudopotential deeper, the en-

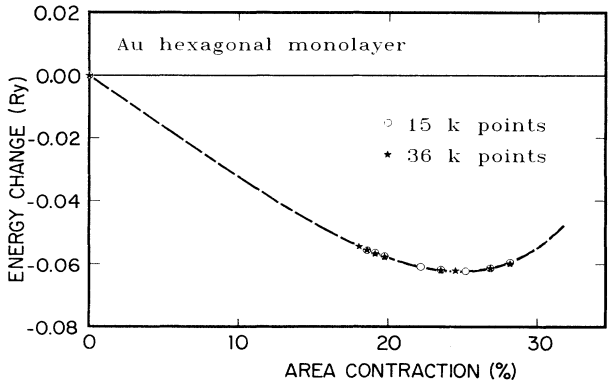

FIG. 2. Energy change per atom for the Au hexagonal monolayer as a function of the percentage contraction of surface area per atom for two different numbers of **k** points.

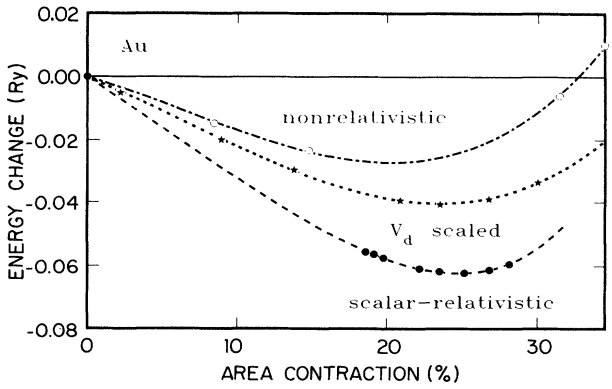

FIG. 3. Energy change per atom of the Au hexagonal monolayer as a function of the percentage area contraction using a nonrelativistic pseudopotential, and a pseudopotential with the d part increased by 5%. The results with the scalar relativistic potential are shown for comparison.

ergy gained by the Au monolayer when contracting is reduced. The more extended nature of the $5d$ states and the stronger bonding through hybridization can be traced further to relativistic effects and the bigger core of Au. The bigger core of $5d$ metals forces the d states further away from the nucleus; the relativistic effects lower the energy of the s states and enhance hybridization. In a previous calculation[21] we have shown that the bulk properties of nonrelativistic Au bear a close resemblance to the properties of Ag. To illustrate this point further, we study the energetics of the Au hexagonal monolayer using a nonrelativistic pseudopotential. In Fig. 3 we can see that the energy gained by the Au monolayer during contraction is substantially reduced when the calculation is done with a nonrelativistic rather than the scalar relativistic pseudopotential. In fact, the curve obtained for nonrelativistic Au is very similar to that of Ag.

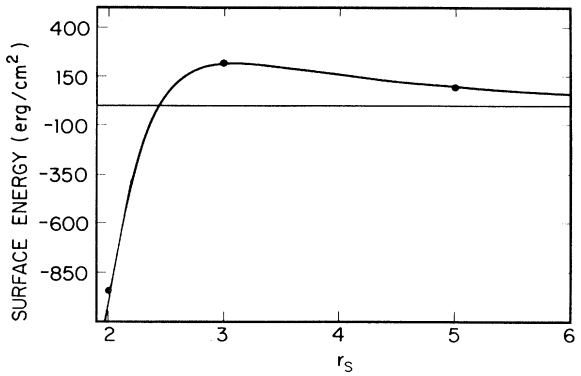

FIG. 4. The surface energy of jellium calculated with the slab geometry compared with the results in Ref. 28.

IV. Ag AND Au MONOLAYERS OF JELLIUM

In the monolayer calculations we have presented, the Au layer transforms by itself, but in reality, the top layer on Au(100) has a substrate of atoms underneath. It is important to investigate the effect of the substrate on the transformation of the top layer. The best way to include the substrate effect without losing the translational symmetry (so that the conventional first-principles techniques can be applied) is to substitute the Au (or Ag) substrate by a jellium slab, in which the positive ionic charges are spread uniformly and have density,

$$n_+(\mathbf{r})=n\ , \quad |z|\le a/2$$
$$=0\ , \quad |z|>a/2\ , \tag{2}$$

where n is constant, and a is the thickness of the jellium slab. The ionic potential due to this jellium background is the Coulomb potential due to the repeated slabs (supercell geometry) of this uniform charge. The d band is nominally full in noble metals, so directional effects in the d bonding are small. A jellium slab of appropriate charge density is hence a reasonable representation of the influence of the substrate. The r_s value of the jellium slab should be chosen so that atoms placed on top of the jellium slab experience a similar environment as those placed on top of a real substrate. In this respect, r_s can be determined in two ways. (i) Take the charge density in interstitial positions, midway between two nearest neighbors in the bulk. This method gives $r_s=1.8$ and 2.0 for Au and Ag, respectively. (ii) Put a monolayer over a jellium slab and vary the charge density of the jellium until the charge profile averaged along the (100) direction (solved self-consistently) on the monolayer matches that of the top layer in the real slab calculation (monolayer on real Au or Ag). This gives $r_s=1.6$ and 1.7 for Au and Ag, respectively. Results for both choices of r_s will be presented below.

As a check, we first compute using the slab geometry the surface energy for a few jellium densities and compare with the values found by Lang and Kohn[28] in Fig. 4. The agreement is good. We than repeat the calculation of the energetics of a monolayer, now placed on top of a jellium slab, with jellium densities chosen as described above. The distance of the monolayer from the jellium-slab edge is determined by energy minimization. The calculations were done for the cases of square and hexagonal Au and Ag monolayers on jellium, and the energies are calculated as a function of the area of the surface unit cell. The total energy of the system now includes the self-energy of the jellium, which needed to be subtracted because we are primarily interested in the intralayer interaction under the influence of the substrate, not the energy of the substrate itself. The results are then fitted in the form of the universal binding curves and plotted as energy change versus percentage area contraction of the layer, using the ideal (100) surface as a reference, in Fig. 5(a) for Au and 5(b) for Ag, respectively.

In Figs. 5(a) and 5(b), the jellium densities for both Au and Ag are taken to be $r_s=1.9$, which is chosen according to the first method (interstitial density). When we compare Fig. 5 with Fig. 1, we notice that for all cases considered, the energy gain due to contraction is smaller than the energy gain when the monolayer is in isolation. Except for an overall reduction in the energy scale, the jellium results are qualitatively similar to those of the monolayer: The hexagonal structure is more energetically favorable than the square for both Au and Ag, and Au gains more energy in contraction.

In Fig. 6 we plot the relative energy change as the Au and Ag hexagonal monolayers contract with $r_s=1.6$ for Au and $r_s=1.7$ for Ag (i.e., r_s is chosen using the second method to determine the jellium density). The results are again qualitatively the same, showing that our conclusions are not dependent on the exact value of r_s chosen.

We have checked the $\mathbf{k}$-point convergence of the monolayer on jellium calculations by increasing the number of $\mathbf{k}$ points from 15 to 28 for the case of Au monolayer of jellium with $r_s=1.6$. The curve with less $\mathbf{k}$ points is more noisy, but the two fitted curves are virtually indistinguishable.

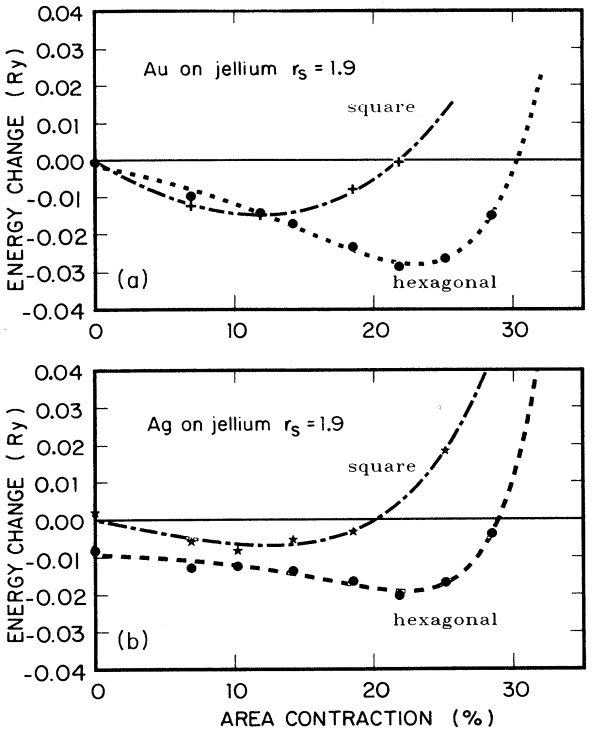

FIG. 5. Energy change per atom for square- and hexagonal-Au monolayers on top of jellium ($r_s=1.9$) as a function of the percentage area contraction for (a) Au and (b) Ag.

In the above calculations, the thickness of the jellium slab is 11.6 a.u. (corresponding to the thickness of three layers of Au or Ag), and the size of the unit cell in the (100) direction is about 31.0 a.u. To see the dependence of our calculations on the thickness of the jellium, we repeated the calculation with a slab thickness of 13.5 a.u. (three and one-half layers of atoms) for the case of Au with $r_s=1.6$, and the results are pretty much the same (see Fig. 7).

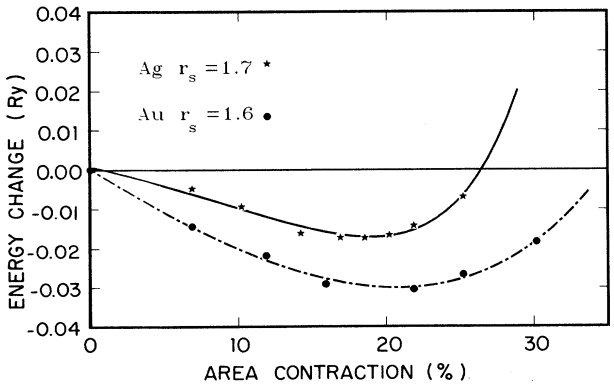

FIG. 6. The energy change per atom for hexagonal-Au and -Ag monolayers on jellium ($r_s=1.6$ for Au and 1.7 for Ag) as a function of the percentage area contraction per atom.

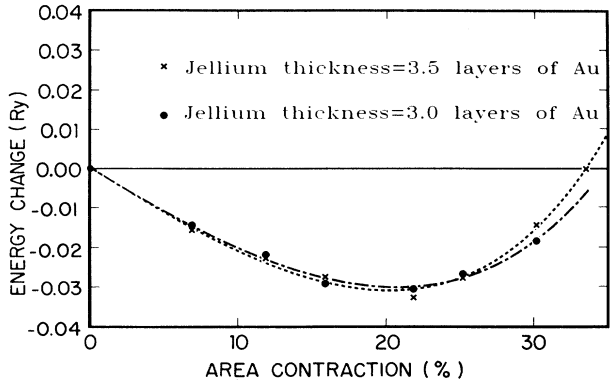

FIG. 7. The energy change per atom for hexagonal-Au monolayers on jellium ($r_s=1.6$) as a function of the percentage area contraction per atom for two different thicknesses of the jellium slab.

V. SLAB CALCULATIONS

For the top layer of the (100) surface to undergo a contractive reconstruction to a hexagonal-close-packed structure, the energy gained by contracting must be greater than the energy it loses due to a loss of registry with the underlying layers (the "mismatch energy"). This mismatch energy was not present in the monolayer-jellium calculations because the jellium substrate is uniform. Atoms on the ideal (100) surface are all positioned at the lowest-energy fourfold site. After the transformation to a denser hexagonal arrangement, this will no longer be true, so the mismatch energy is basically the energy for the top-layer atoms to occupy general surface positions rather than the lowest-energy fourfold sites. To take this effect into account, we express the interaction energy between the atoms on the top layer and the underlying substrate in terms of a periodic potential depending on the positions occupied by the top-layer atoms; then,

$$E_{\text{mismatch}}=\sum_i V(R_i)\ ,$$
$$V(R)=\sum_G W_G e^{iG\cdot R}\ , \tag{3}$$

where the G's are the two-dimensional (2D) reciprocal lattice vectors of the (100) surface and $R_i=(x_i,y_i)$ is the position of an atom on the top layer. Terminating this equation beyond the lowest order, we obtain

$$V(x,y)=V_0+\frac{W}{4}\left[\cos\frac{2\pi}{a}x+\cos\frac{2\pi}{a}y\right]\ , \tag{4}$$

where a is the lattice constant of the 2D square substrate lattice. The constant W can be obtained from the energy difference between the energy of top-layer atoms at the lowest-energy fourfold site [$R=(0,0)$] and the highest-energy site [$R=(a/2,a/2)$], which is the atop site. The calculations are again done with the repeated slab geometry. The slabs are five layers thick, separated by a vacuum of about 15.5 a.u. The total energy of the slab with the surface layer atoms occupying the fourfold site

[E(fourfold)] and the slab energy with the surface layer atoms at the atop site [E(atop)] are calculated. The constant W is then given by $W=\frac{1}{2}[(E(\text{atop})-E(\text{fourfold})]$, where the factor $\frac{1}{2}$ takes care of the fact there are two surfaces in a slab. For both the ideal geometry and the slab with its surface layer shifted, all the interlayer distances are fully relaxed until the forces[29] are negligibly small. This is important because the relaxation is large for the case of the surface layer at the atop site (see Table I). The values of W are found to be 36.8 and 39.3 mRy per surface atom for Au and Ag, respectively. A plot of this potential energy for Au according to Eq. (4) is shown in Fig. 8. Our results indicate that Au actually has a slightly smaller mismatch energy than Ag, while it gains quite a bit more energy than Ag on contracting. This is the reason why Au(100) reconstructs and Ag(100) does not.

From the ideal fully relaxed slab calculation, we can also obtain the surface energy of the (1×1) surface, which is also an important factor in determining the energetics of the transformation. We have $E_s=\frac{1}{2}(E(\text{slab})-nE_{\text{bulk}})$, where E_s is the surface energy per surface atom, n is the number of layers in the slab, E(slab) is the total energy of the fully relaxed slab, E_{bulk} is the energy per atom in the bulk, and the factor $\frac{1}{2}$ is again due to the existence of two surfaces in a slab. We found $E_s=51.5$ mRy per surface atom for Au and $E_s=42.9$ mRy for Ag. This gives surface energy values of 1.33 J/m^2 for Au, and 1.11 J/m^2 for Ag. The values agree well with the surface tension values given by Somorjai[30] ($\gamma=1.41$ J/m^2 for Au and $\gamma=1.14$ J/m^2 for Ag).

We repeat the calculations for Au with a seven-layer slab and find $W=36.5$ mRy and $E_s=52.3$ mRy, respectively, in good agreement with the results obtained with the five-layer-slab calculations. In Table I we show the percentage change of the interlayer distances in the fully relaxed geometry with the top layer occupying the fourfold site and the atop site, respectively. The differences between the five- and seven-layer-slab results are again small. It can be seen from Table I that relaxation is small when the top-layer atoms occupy the fourfold sites, but there is a 30% outward relaxation if the top-layer atoms occupy the atop sites. Since both of these sites are occupied on the reconstructed Au(100) surface, a corrugation of the top layer is expected. This corrugation can be estimated by the difference in the heights of the top-layer atoms at the fourfold (lowest) position and the atop site (highest) position. Our calculations give a peak-to-peak corrugation of about 0.6 Å, which agrees with the experimental value of 0.5 Å found by Rieder *et al.* using He scattering.[2] The average position of the top layer above the second layer should also be quite a bit higher for the reconstructed surface than for the unreconstructed (100) surface.

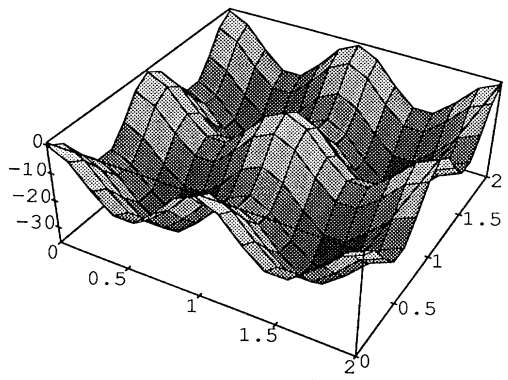

FIG. 8. A three-dimensional plot of the interaction energy between the substrate and the top-layer atoms for Au(100).

TABLE I. Change of interlayer separations in percentage of the inner layer separation for different sizes of the slab for Au(100) with the top-layer atoms at the fourfold site and atop site. Positive numbers indicate an increase in the interlayer separation.

	Five layers of Au		Seven layers of Au	
	fourfold	atop	fourfold	atop
Δ_{12}	−2.4	32.8	−2.1	29.0
Δ_{23}	0.0	0.0	0.0	−1.0

VI. FRENKEL-KONTOROWA SIMULATION

To investigate in more detail the competition between the intralayer forces and the substrate potential in determining the structure of the top layer, we employ a simple model in which we express the energy of the system as a sum of two terms depending on the coordinates of the top-layer atoms:

$$E=\sum_{ij} e(R_i-R_j)+\frac{W}{4}\sum_i\left[\cos\frac{2\pi}{a}x_i+\cos\frac{2\pi}{a}y_i\right], \tag{5}$$

where $R_i=(x_i,y_i)$ is the position of the ith surface atom, and a is the lattice constant of the unreconstructed (100) surface.

The first term describes the in-plane interaction of the monolayer in the presence of the substrate, while the second term includes the effect of the registry imposed by the substrate. The values of W were determined for both Au and Ag in Sec. VI. In the first term the two-body potential functions (e) are determined by fitting to our hexagonal monolayer on jellium calculations (with $r_s=1.9$ for both Au and Ag). This model is very similar to the model originally proposed by Frenkel and Kontorowa,[31] (FK) although the original formulation was one-dimensional, and the interaction (e) was taken to be harmonic springs with a unique force constant. The ground-state structure of the system is determined by a competition between the intralayer strain energy (first term), which favors a contracted layer, and the substrate potential (second term), which tries to pin the atoms in registry with the underlying uncontracted layers. In the ground state, the atoms will rearrange in such a way that there is an equilibrium between the strain energy and the potential energy so that the total energy is minimum.

While the one-dimensional FK model can be solved analytically in the continuum limit,[31] to find the ground state of the two-dimensional case we have to use numerical techniques. In our calculations, a 2D mesh of 61×61 atoms is used. Molecular dynamics can be used to find directly the ground-state configuration, but since we want to monitor the surface energy change as the top layer contracts, we go through the slightly more tedious procedure of finding the lowest-energy configuration for a series of fixed surface densities. The atoms in the 2D mesh are placed in an initially perfect hexagonal arrangement, with the average surface density constrained to correspond to a given contraction. This can be done conveniently be fixing the boundary atoms while letting the other atoms relax. The positions of the atoms $R_i's$ are relaxed by a steepest-descent procedure until we reach a configuration that gives a local energy minimum. At each step, we calculate the forces acting on each particle, and the atoms are displaced in the direction of the forces by an amount proportional to the magnitude of the forces. The proportionality constant λ is chosen so as to minimize the total energy of the mesh. We repeat this procedure until the force on each atom is zero.

From our model simulations, we can obtain the energy change per surface atom as the top layer transforms from a square arrangement in registry with the substrate to a contracted hexagonal arrangement. However, since the density of atoms on the surface changes in the process, the proper quantity that governs the reconstruction is the change in surface energy. The change in the total surface energy for a given amount of contraction can be written as

$$D(q)=N[d(q)+qE_s]/(1-q)\ , \tag{6}$$

where q is the fractional decrease in area per surface layer atom ($q=0$ at the ideal surface), $d(q)$ is the energy change per surface atom as the top layer transforms from square to hexagonal obtained from our simulations, E_s is the surface energy of a fully relaxed (1×1) surface, N is the total number of atoms on the unreconstructed surface. This equation can be obtained directly by comparing the total surface energies of the system before and after a contraction, keeping the definition of $d(q)$ in mind. The term containing E_s resolves the fact that when the top layer contracts and gains an amount of energy $d(q)$, a total of Nq atoms from the substrate will be exposed. The denominator resolves an increase in the surface density by $1/(1-q)$ in the final product. Alternatively, the denominator can be regarded as a renormalization factor: While the top layer contracts, exposing some underlying layer atoms, the exposed atoms can also contract to further reduce the surface energy. The process can go on and on, leading to a total renormalization factor of $1/(1-q)$.

Once $d(q)$ is found, Eq. (6) can be used to find the change of the surface energy as a function of q. Results are ploted in Fig. 9 for Au and Ag. It is energetically favorable for Au to reconstruct but not for Ag. The area contraction for Au is around 21%, which agrees very well with experiments (20%). The atomic arrangements

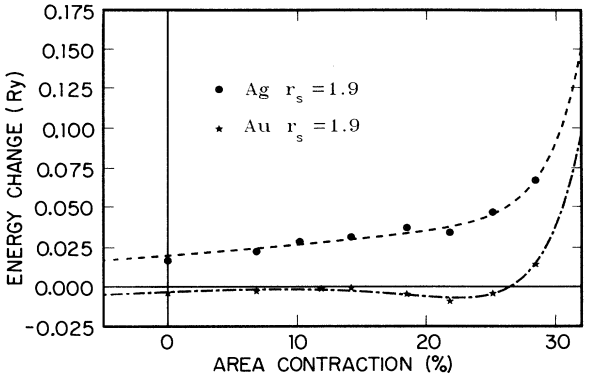

FIG. 9. Surface energy change (per surface site) for Au and Ag as a function of the percentage area contraction.

in the minimum-energy configuration is shown in Fig. 10. The Au layer is basically hexagonal, distorted somewhat by the underlying potential.

Recent x-ray diffraction experiments,[13] in agreement with earlier studies,[5,8,10] found that the hexagonal top layer of Au(100) is slightly rotated with respect to the substrate. The Frenkel-Kontorowa-type model used in our simulations can in principle handle any kind of surface layer transformation, but in practice, it is good for determining transformation of a local length scale and is not practical for the study of rotation domains of mesoscopic (or macroscopic) scale. This is because the simulation cell employed has to be significantly larger than the domain size, unless we already know beforehand the domain size and the domain wall structures. Rotational transformations are also very likely to possess many local minima, and more computationally intensive schemes like simulated annealing have to be used for the simulation if one wishes to pursue this problem further.

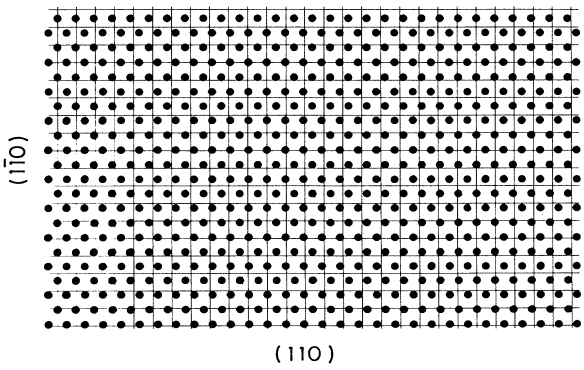

FIG. 10. The reconstructed Au(100) surface as given by the Frenkel-Kontorowa model. The solid circles indicate the position of atoms in the reconstructed top layer. The intersections of the lines show the atom positions in the second layer.

VII. CONCLUSIONS

We have applied first-principles calculations together with modeling techniques to show that it is energetically favorable for the top layer of Au(100) to reconstruct, changing from a square lattice to a contracted hexagonal-close-packed structure, while the top layer of Ag(100) does not. We found that the main driving force behind the Au(100) reconstruction is the strong tendency for the top layer to go to a more compact arrangement, so strong that it can overcome the energy loss by losing registry with the substrate underneath. For Ag, the top layer is also hexagonally inclined, but the energy gained in such a transformation is not large enough to overcome the substrate potential, so the surface stays unreconstructed. This difference is due mainly to a stronger participation of the *d* orbitals in the bonding of Au than Ag, which in turn can be traced to the fact that Au has a higher atomic number and therefore a bigger core and stronger relativistic effects. These differences are not specific to Ag and Au. Hence it is not surprising that similar reconstructions occur in the (100) surfaces of the 5*d* fcc metals Ir and Pt but not in the corresponding (100) surfaces of the 4*d* metals Rh and Pd. We believe that this class of reconstruction, involving the transformation of the top layer, can happen whenever the top layer favors an arrangement different from its substrate and the intralayer interactions are dominant over the interlayer interactions. Metal overlayers of one kind over another are prime candidates for such reconstructions. Ag on Cu(100) (Ref. 32) may be another example.

ACKNOWLEDGMENTS

Ames Laboratory is operated for the U.S. department of Energy by Iowa State University under Contract No. W-7405-Eng-82. This work was supported by the Director of Energy Research, Office of Basic Energy Sciences, U.S. Department of Energy (including a grant of computer time on the Cray computers at the Lawrence Livermore Laboratory).

[1]D. G. Fedak and N. A. Gjostein, Acta Metall. **15**, 827 (1967).
[2]K. H. Rieder, T. Engel, R. H. Swendsen, and M. Manninen, Surf. Sci. **127**, 223 (1983).
[3]D. G. Fedak and N. A. Gjostein, Surf. Sci. **8**, 77 (1967).
[4]M. A. Van Hove, R. J. Koestner, P. C. Stair, J. P. Biberian, L. L. Kesmodel, I. Bartos, and G. A. Somorjai, Surf. Sci. **103**, 189 (1981).
[5]G. K. Binning, H. Rohrer, Ch. Gerber, and E. Stoll, Surf. Sci. **144**, 321 (1984).
[6]G. Binning, H. Rohrer, Ch. Gerber, and E. Weibel, Surf. Sci. **131**, L379 (1983).
[7]J. Perdereau, J. P. Biberian, and G. E. Rhead, J. Phys. F **4**, 798 (1974).
[8]H. Melle and E. Menzel, Z. Naturforsch. Teil A **33**, 282 (1978).
[9]J. C. Heyraud and J. J. Metois, Surf. Sci. **100**, 519 (1980).
[10]K. Yamazaki, K. Takayanagi, Y. Tanishiro, and K. Yagi, Surf. Sci. **199**, 595 (1988).
[11]U. Harten, A. M. Lahee, J. Peter Toennies, and Ch. Woll, Phys. Rev. Lett. **54**, 2619 (1985).
[12]Ch. Woll, S. Chiang, R. J. Wilson, and P. H. Lippel, Phys. Rev. B **39**, 7988 (1989).
[13]D. Gibbs, B. M. Ocko, D. M. Zehner, and S. G. J. Mochrie, Phys. Rev. B **42**, 7330 (1990); S. G. J. Mochrie, D. M. Zehner, B. M. Ocko, and D. Gibbs, Phys. Rev. Lett. **64**, 2925 (1990).
[14]F. Ercolessi, M. Parinello, and E. Tossatti, Phys. Rev. Lett. **57**, 719 (1986).
[15]B. W. Dodson, Phys. Rev. B **35**, 880 (1987).
[16]N. Takeuchi, C. T. Chan, and K. M. Ho, Phys. Rev. Lett. **63**, 1273 (1989).
[17]D. R. Hamman, M. Schluter, and C. Chiang, Phys. Rev. Lett. **43**, 1494 (1979); G. B. Bachelet and M. Schluter, Phys. Rev. B **25**, 2103 (1982); L. Kleinman, *ibid.* **21**, 2630 (1980).
[18]P. Hohenberg and W. Kohn, Phys. Rev. **136**, B864 (1964); W. Kohn and L. J. Sham, *ibid.* **140**, A1133 (1965).
[19]L. Hedin and B. I. Lundqvist, J. Phys. C **4**, 2064 (1971).
[20]S. G. Louie, K. M. Ho, and M. L. Cohen, Phys. Rev. B **19**, 1774 (1979).
[21]N. Takeuchi, C. T. Chan, and K. M. Ho, Phys. Rev. B **40**, 1565 (1989).
[22]K. M. Ho and K. P. Bohnen, Phys. Rev. Lett. **59**, 1833 (1987).
[23]N. Takeuchi, C. T. Chan, and K. M. Ho (unpublished).
[24]S. L. Beauvais, R. J. Behm, S. L. Chang, T. S. King, C. G. Olson, P. R. Rape, and P. A. Thiel, Surf. Sci. **189/190**, 1069 (1987).
[25]S. G. Louie and M. L. Cohen, Phys. Rev. B **13**, 2461 (1976).
[26]J. H. Rose, J. Ferrante, and J. R. Smith, Phys. Rev. Lett. **47**, 675 (1981).
[27]See, e.g., J. F. Annett and J. E. Inglesfield, J. Phys. Condens. Matter **23**, 3645 (1989).
[28]N. D. Lang and W. Kohn, Phys. Rev. B **1**, 4555 (1970).
[29]H. Hellman, *Einführung in die Quantenchemie* (Deuticke, Leipzig, 1937); R. P. Feynman, Phys. Rev. **56**, 340 (1939).
[30]G. A. Somorjai, *Chemistry in Two-Dimensions: Surfaces* (Cornell University Press, Ithaca, NY, 1981), p. 31.
[31]J. Frenkel and T. Kontorowa, Phys. Z. Sowjetunion **13**, 1 (1938); F. C. Frank and J. H. Van der Merwe, Proc. R. Soc. London, Ser. A **198**, 205 (1949).
[32]P. W. Palmberg and T. N. Rhodin, J. Appl. Phys. **39**, 2425 (1968); J. Chem. Phys. **49**, 134 (1968); **49**, 147 (1968).